

Algorithm Maintenance and Validation of MODIS Cloud Mask, Cloud Top-Pressure, Cloud Phase and Atmospheric Sounding Algorithms

Contract number: **NNX14AN48G**

Activities: June 2016 – May 2017

UW-Madison Investigators:

S. A. Ackerman (PI)	W. P. Menzel
B. Baum	E. Borbas
R. Frey	C. Moeller

Table of Contents

Introduction	2
MODIS Calibration Activities	2
Terra MODIS PVLWIR Crosstalk.....	2
Terra MODIS Destriping Configuration File Update.....	5
Cloud Mask (MOD35/MYD35).....	8
Atmospheric Profiles (MOD07/MYD07).....	10
Terra and Aqua Comparison.....	10
Cloud Top Heights and Phase (MOD06/MYD06)	14
MODIS Collection Pixel Level Comparison.....	16
Work Plan.....	17
References	18
Publications.....	19
Meetings	20

Introduction

The goal of this work is to maintain, validate and refine four Terra and Aqua MODIS algorithms: cloud mask (MOD35/MYD35) and associated clear sky composite maps, atmospheric profiles (MOD07/MYD07), cloud top properties (CTP) including cloud-top pressure, temperature, and phase (part of MOD06/MYD06). Maintenance requires (a) monitoring changes in calibration and associated adjustment of cloud detection thresholds, (b) considering replacement channels when primary channels exhibit calibration problems, and (c) continuing validation through comparisons with products from other satellite based algorithms, ground-based observations and focused field experiments.

The team has focused on monitoring results and processes associated with of Collection 6 code. This is accomplished through comparison with other satellite-derived products as well as surface based platforms and through monitoring trends. The team also interacts with the MODIS processing team as they make modifications to the processing stream or ancillary data.

MODIS Calibration Activities

Terra MODIS PVLWIR Crosstalk

The Terra MODIS Photovoltaic (PVLWIR) bands 27-30 are known to experience an electronic crosstalk contamination that has resulted in a longterm drift in the radiometric bias of these bands. The drift has compromised the climate quality of Terra MODIS L2 products that depend significantly on these bands, including cloud mask (MOD35), cloud fraction and cloud top properties (MOD06), and total precipitable water (MOD07). A crosstalk mitigation strategy was developed and tested by MCST with Wisconsin providing reviews and feedback on the strategy and efficacy of the various versions of the crosstalk correction. A linear crosstalk correction algorithm using band averaged influence coefficients based upon monthly lunar views by Terra MODIS has been adopted through this effort for implementation in the operational L1B processing algorithm (Wilson et al. 2017).

At the L1B level, Wisconsin has generated case studies to test the efficacy of the crosstalk correction. Using Terra MODIS L1B granules from 2001-2015 (pre safe mode) and 2016 (post safe mode), Wisconsin has compared crosstalk corrected radiances from those of Terra MODIS to L1B from Aqua MODIS, which is largely believed to have little or no impact from electronic crosstalk for the PVLWIR bands. These case studies demonstrated that Terra MODIS calibrated radiances are brought significantly closer to those of Aqua MODIS

by applying the crosstalk correction (Figure 1). While the crosstalk correction brings the Terra MODIS data much closer to that of Aqua MODIS, some residual influence appears to remain, as suggested by the plot for 2015 in Figure 1. This residual influence is also present in case studies using Terra MODIS data after the February 2016 safe mode event. These residuals will continue to be monitored with time to reveal any trends that may be present in the crosstalk corrected L1B data.

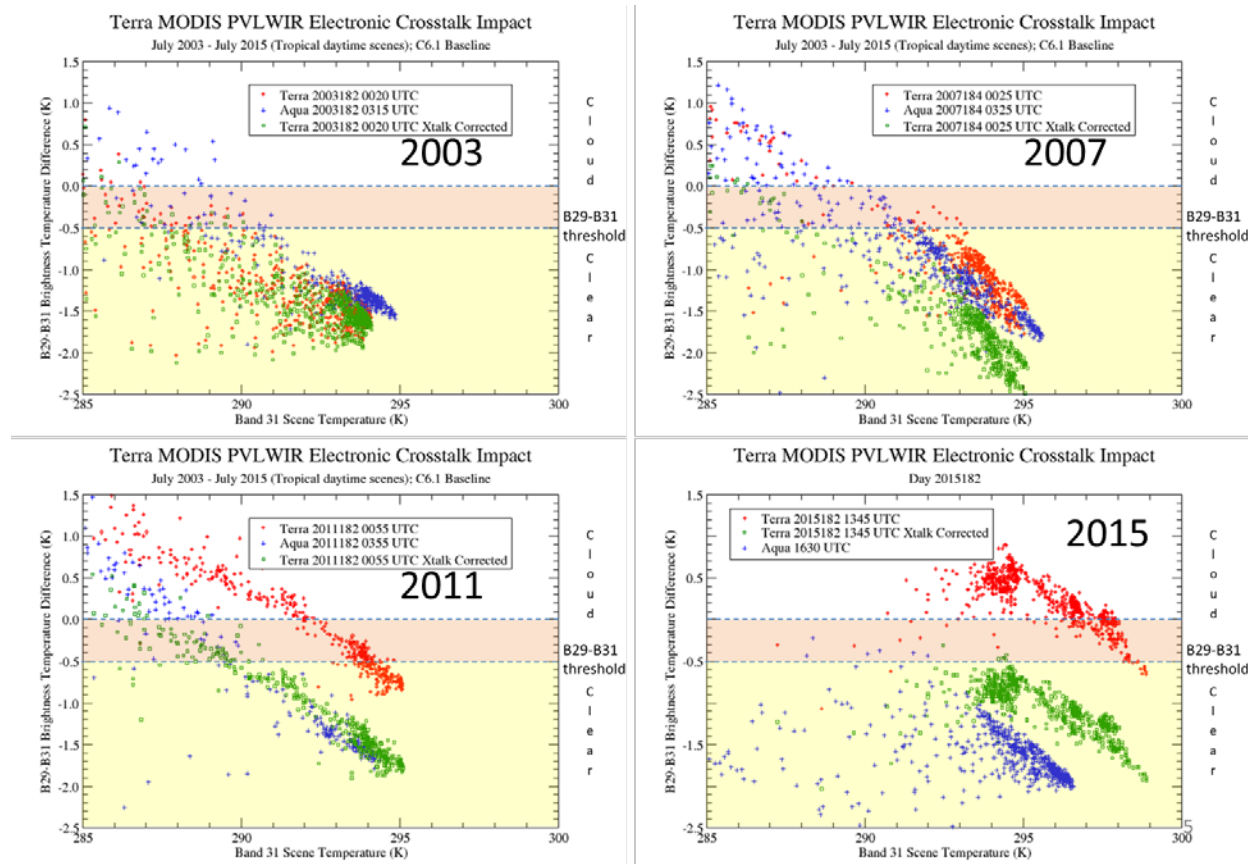


Figure 1 Terra MODIS B29-B31 difference snapshot for a granule in each of four years. 2003 shows little evidence of crosstalk as Terra (red) and Aqua (blue) data closely match. But as the mission continues, Terra and Aqua diverge. Crosstalk correction of Terra data (green) improves the agreement with Aqua.

Additionally, applying the crosstalk correction significantly reduces striping in the MODIS L1B product of the PVLWIR bands (Figure 2). This is especially true for bands 27 (B27) and 28 (B28) as striping of nearly 10 K is reduced to about 1 K; band 29 (B29) striping is reduced from about 1.5 K down to about 0.5 K by the correction.

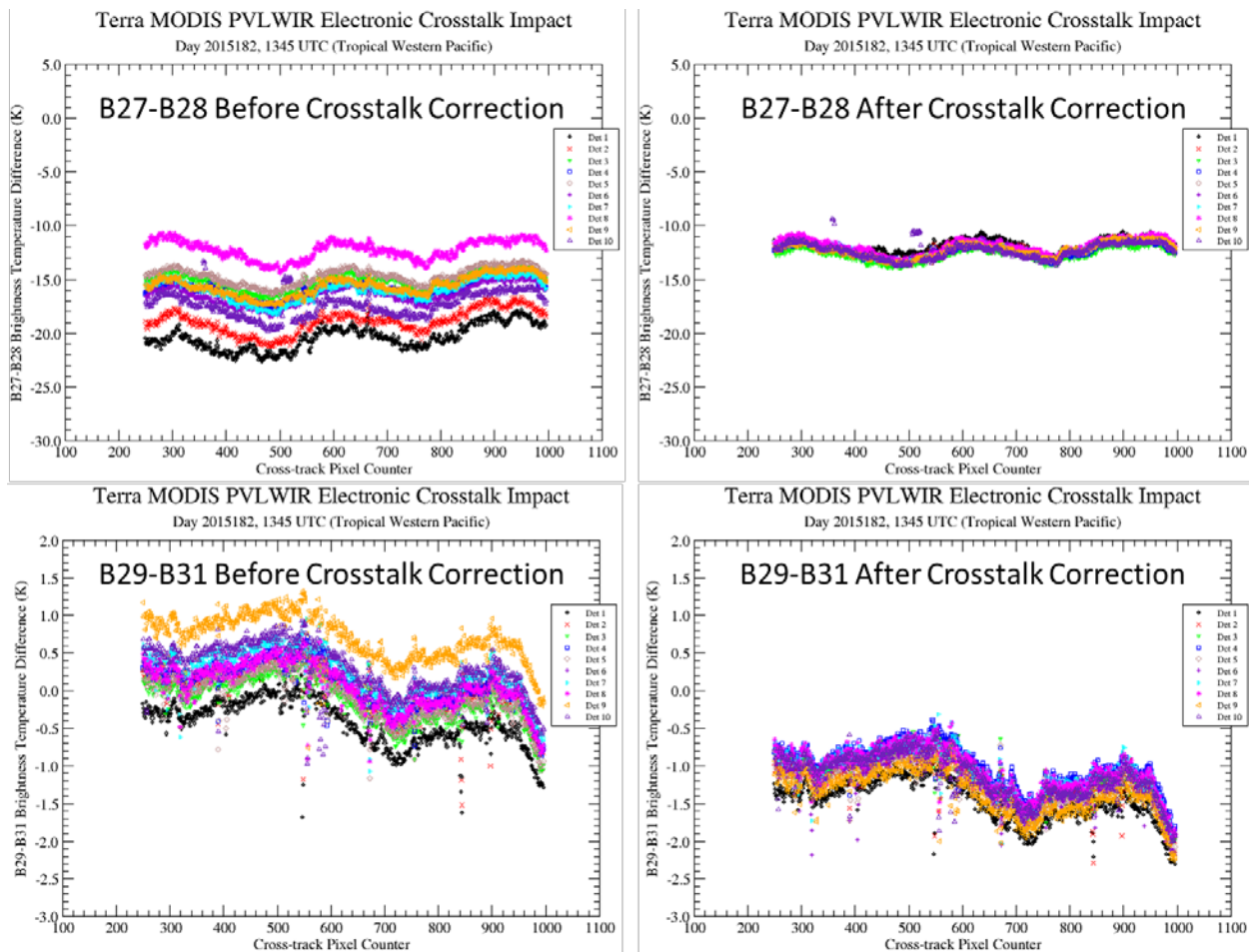


Figure 2 Snapshot of Terra MODIS B27-B28 (top row) and B29-B31 (bottom row) differences before crosstalk correction (left column) and after crosstalk correction (right column). Note scale differences between top row and bottom row. Detector striping is greatly reduced in all bands by the application of the crosstalk correction.

Simultaneous Nadir Overpasses (SNO) between Terra and MetOp-A provide an opportunity to assess MODIS calibration against the well-calibrated hyperspectral IASI instrument, which has overlapping spectral coverage with MODIS crosstalk impacted PVLWIR bands. SNO comparisons before and after applying the crosstalk correction for April of the years 2008 – 2016 show the impact of the correction on Terra MODIS radiance biases and trends in those biases. Before applying the crosstalk correction (Figure 3), the bias averaged into 10 K temperature bins (green circles, upper plots) for all four bands shows varying levels of dependence upon scene temperature, exhibiting slopes and curvature in the plots. By contrast, the average bias for band 31 (B31), which is unaffected by crosstalk, shows essentially no dependence on scene temperature. Bias trends easily exceed 1 K in B27 and B30 over the eight year period (red circles, lower plots) for the cold high latitude scenes of the Terra and MetOp-A SNOs. These biases are expected to be much larger over warm tropical scenes. The sharp increase in the B27 bias for April 2016 is a result of a significant change in B27 detector performance after a shutdown of the MODIS instrument during the

February 2016 Terra safe mode event. That safe mode event also caused a significant increase in electronic crosstalk for all PVLWIR bands (Wilson et al., 2017). B28 and B29 show smaller trends of about 0.5 K over the eight year period. Although these trends are smaller, they nevertheless significantly impact L2 products. The trends in all PVLWIR bands are indicative of an increase in electronic crosstalk over the period. Further, evidence from L2 products suggests that these trends are significantly larger in warm scenes such as exist in the low latitudes of the tropical zone.

After applying the crosstalk correction in the L1B algorithm, the MODIS biases and trending are significantly reduced (Figure 4). The largest improvement occurs at the warmer scene temperatures with only modest impact for cold, low signal, scenes. The scene dependence of MODIS biases is greatly reduced in all bands, most dramatically in B27 where biases of several degrees with a large scene temperature dependence are reduced to less than 0.5 K with minimal scene dependence. The scene dependence in all the PVLWIR bands after the crosstalk correction is more linear and much more closely matches that of B31. Bias trends over time are also generally reduced, most notably in B27 where the trend reduces from about 2 K for these SNO scenes down to about 0.5 K over the eight year period. The band 30 trend, while significantly reduced by the correction, is still about 1.0 K, suggesting that the crosstalk correction is not as effective for this band as for the other PVLWIR bands.

Terra MODIS Destriping Configuration File Update

As seen in Figure 2, the crosstalk correction causes a significant reduction in detector striping and has also resulted in several detectors previously assigned a status of “Noisy” to return to good performance. In light of this, a review of the Terra MODIS destriping algorithm configuration files for the entire mission was undertaken and updates have been provided to MODAPS for implementation. The original set of four destriping configuration files to cover the complete Terra MODIS mission has been expanded to 21 configuration files which better capture variation in the Terra MODIS detector performance. An improvement in the destriped L1B product will benefit the MODIS Cloud Mask (MOD35), Cloud Top Properties (MOD06), and Atmospheric Profiles (MOD07) L2 products.

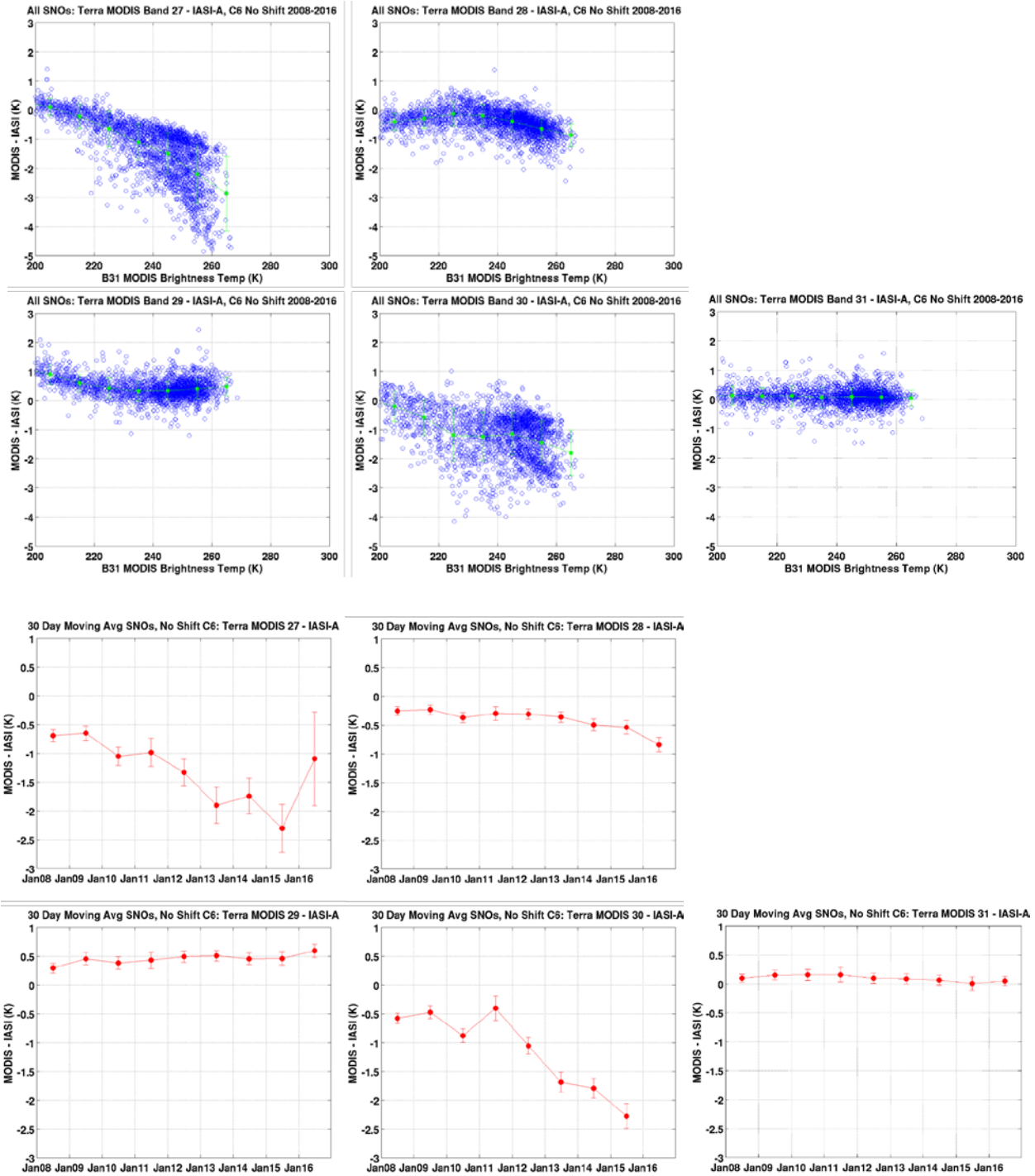


Figure 3 Terra MODIS - MetOp-A IASI SNO comparisons for bands 27-30 before crosstalk correction of MODIS L1B radiances. Band 31 plots provided for reference as a band that is not affected by crosstalk. Upper plots show MODIS bias as a function of scene temperature. Lower plots show MODIS bias as a function of time.

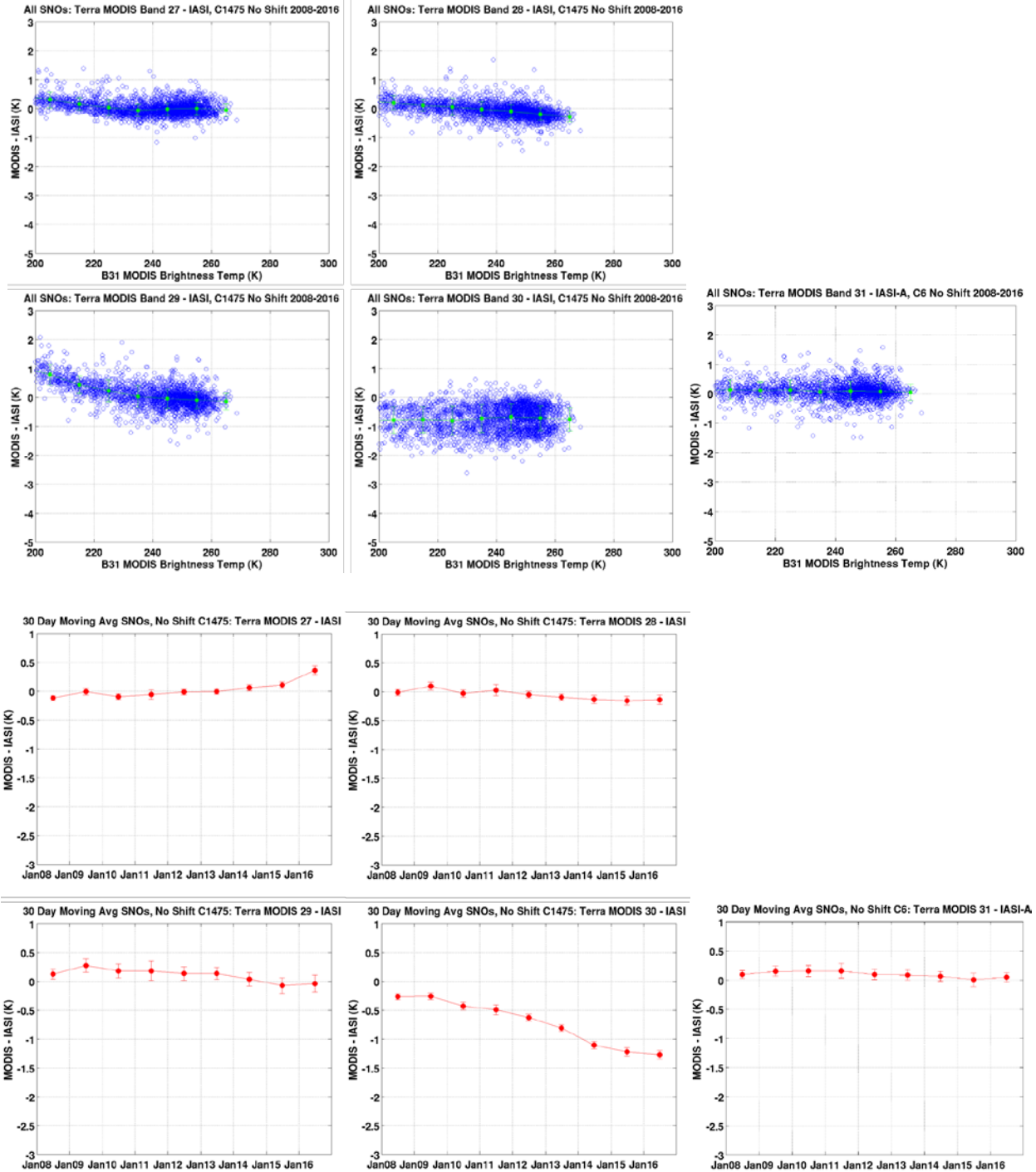


Figure 4 Same as Figure 3 except after crosstalk correction of MODIS L1B radiances. Crosstalk correction greatly reduces scene dependence and trends in bias.

Cloud Mask (MOD35/MYD35)

Activities related to the MODIS cloud mask (MOD35) centered on the 8.6 μm (band 29) calibration issue that was noted in the previous annual report. The slow warming of observed brightness temperatures (BTs) in this atmospheric water vapor absorption band increased the numeric value of an 8.6 minus 11.1 μm brightness temperature difference (BTD) used in the algorithm to detect ice clouds over water surfaces. Over time, the confidence of clear sky reported by this cloud test began to lessen in actual clear sky scenes and impacted the cloud mask final result: first to probably clear, then to probably cloudy, and finally to confident cloud in some cases. This is illustrated in Figure 5 where the fraction of confident clear pixels from 60S-60N over oceans is plotted as a function of time (trend). One sees a decrease beginning in about 2011 but then a sharp decrease from about 2013. The variability in the clear fraction (observed) also decreases after this date, indicating that cloud vs. clear discrimination has become severely compromised in oceanic regions of the world.

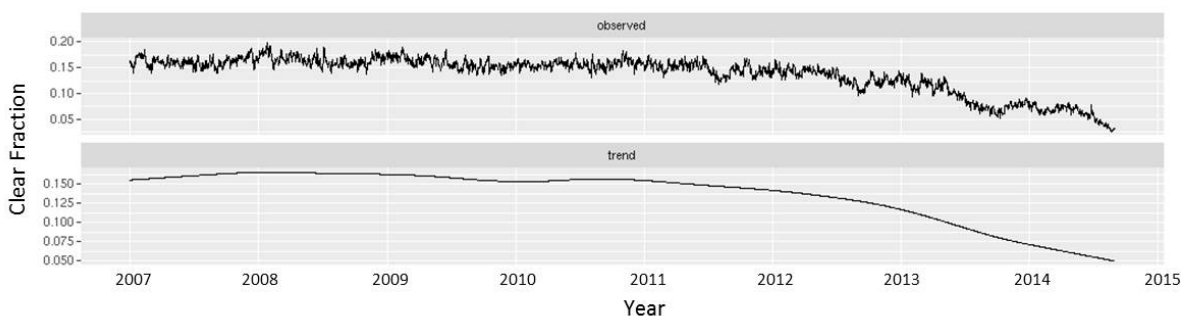


Figure 5 Fraction of confident clear pixels in the MODIS cloud mask (MOD35) as a function of time, from 60S to 60N latitude, water surfaces only.

During the past year, an electronic crosstalk correction was made to the calibration algorithm for bands 27-30 that greatly improves the performance of the cloud mask. An example of the change in the 8.6 – 11.1 BTD test and resulting output cloud mask is shown in Figure RAF2. Parts a and b show 11.1 and 13.9 μm imagery, respectively, from this nighttime scene located in the tropical eastern Pacific. Parts c and d are depictions of the 8.6 – 11.1 BTD test where the white areas indicate confidence of clear sky < 0.5 (clouds) before and after the calibration correction, respectively. Note that the cloudy regions in part d correspond closely to the 13.9 μm imagery that shows mainly high and presumably ice clouds. Parts e and f are similar to c and d but illustrate changes in the final output cloud mask. Green is clear, blue is probably clear, red is probably cloudy, and white is confident cloudy. The improvement in discrimination between clear and cloudy pixels is dramatic.

Other tests impacted by the calibration changes are the 6.7 μm (band 27) BT high cloud test and polar night 6.7 – 11 μm BTD clear sky restoral test, the polar night 7.3 - 11 μm (band 28 – band 31) BTD cloud test and clear sky restoral test (using different thresholds), and the night ocean 8.6 – 7.3 BTD cloud test. Threshold changes were made to the latter test to

mitigate over-clouding over colder waters. The largest improvement to MOD35 is through the 8.6 – 11.1 BTD test as shown in Figure .

Globally, the 2016 cloudiness experienced only an incremental change (<0.2%) from that of 2015. This conclusion is based on several satellite cloud climatologies including PATMOS-x/AVHRR (Pathfinder Atmospheres Extended/Advanced Very High Resolution Radiometer; Heidinger et al., 2013), Aqua MODIS C6 (Ackerman et al., 2008), CALIPSO (Cloud-Aerosol Lidar and Infrared Pathfinder Satellite Observation; Winker et al. 2007), CERES (Clouds and the Earth’s Radiant Energy System; Minnis et al., 2008; Trepte et al., 2010) Aqua MODIS, MISR (Multi-angle Imaging SpectroRadiometer; Di Girolamo et al., 2010), HIRS (High Resolution Infrared Sounder; Wylie et al., 2005; Menzel et al., 2014), and PATMOS-x/Aqua MODIS. Several of these records: PATMOS-x/Aqua MODIS, CALIPSO, CERES Aqua MODIS, Aqua MODIS C6, and MISR are derived from polar-orbiting satellites flown as part of NASA’s Earth Observing System (EOS). These records are shorter, the earliest starting in 2000, but don’t suffer from issues such as satellite drift or inter-satellite calibration. Figure 6 shows that since 2000 global cloudiness has been relatively stable. The average inter-annual change in cloudiness among all records represented was 0.3% after 2000 and 0.8% before 2000. Currently it is not clear how much of this change is attributable to the influx of records taken from more modern satellites versus actual variability in cloudiness in the 80’s and 90’s. Of the records that extend back before 2000, three of them: PATMOS-x/AVHRR, CLARA-A2 (Cloud, Albedo and Radiation dataset; Karlsson et al. 2017), and SatCORPS (Satellite Cloud and Radiative Property retrieval System; Minnis et al. 2016) are derived from AVHRR instruments flown on NOAA Polar-orbiting Operational Environmental Satellites (POES) and more recently the EUMETSAT MetOP series. Differences among these records can be attributed in part to which satellites were chosen for inclusion in the dataset and how the issue of diurnal drift was addressed, as well as the auxiliary data used in their analyses. The fourth record to extend back before 2000, HIRS, is more focused on the detection of cirrus cloud.

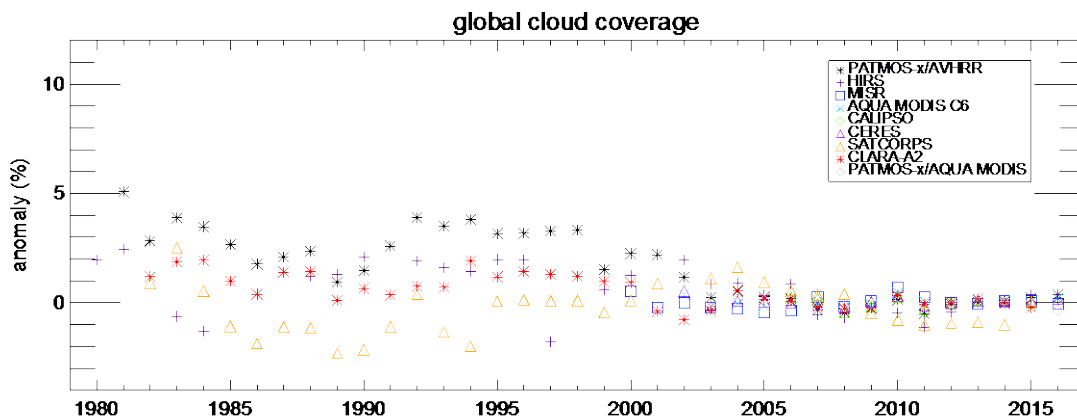


Figure 6 Annual global cloudiness anomalies for 1981-2016. The anomaly is defined as the annual value minus the mean, derived between 2003 and 2015, a period common to the satellite records excluding CALIPSO, where the entire record was used instead. The datasets include (a) PATMOS-x/AVHRR, (b) HIRS, (c) MISR, (d) AQUA MODIS C6, (e) CALIPSO, (f) CERES Aqua MODIS, (g) SatCORPS, (h) CLARA-A2 and (i) PATMOS-x/AQUA MODIS.

IR Cloud Phase and Cloud Top Pressure

Two MODIS atmosphere products were impacted by the drift and subsequent correction in 8.6 and 7.3 μm radiances. The IR cloud phase, found in the MOD06 cloud product files, was severely impacted as far too many clouds were labeled as ice phase. We have determined that the calibration change has fixed the problem with no additional changes necessary. In the CO₂ slicing cloud top pressure algorithm, a ratio of observed minus calculated 8.6 to 11.1 μm radiances (“beta ratio”) is used to screen out unreliable retrievals over water phase clouds. Previous to the calibration correction, too many clouds were determined to be middle or high level (cloud top pressure too low). In this case also, we have determined that the crosstalk correction has mitigated the problem.

Atmospheric Profiles (MOD07/MYD07)

Terra and Aqua Comparison

Collect 6 Terra is compared to Collect 6 Aqua and cross-talk corrected Terra. Figure 7 shows the difference TPW image (downloaded from the LAADS test website) showing that the corrected Terra water vapor MOD07 products were much improved. The quality may still become better when the spectral response function shifts are adjusted for the newly re-calibrated L1B data. The spectral shift test requires a test dataset with Aqua and Terra SNOs along with new MOD07 coefficients. Figure 8 shows the trends from 2002 to the present for the cross-talk corrected Terra TPW, UTH, and LTH in the tropics in April; it is evident that the cross-talk correction is moving the Terra moisture products close to the Aqua determinations (especially for UTH).

MODIS and HIRS moisture determinations were also compared. HIRS TPW and UTH algorithm is a statistical regression modeled on the MODIS algorithm (Seemann et al. 2003) and developed from the SeeBor database (Borbis et al. 2005) that consists of geographically and seasonally distributed radiosonde, ozonesonde, and ECMWF Re-analysis data. TPW & UTH are determined for clear sky radiances measured by HIRS over land and ocean both day and night. There is strong reliance on radiances from 6.5, 11, 12 μm . The AVHRR based PATMOS-x cloud mask is used to characterize HIRS sub-pixel cloud cover. The MODIS and Aqua TPW trends from 2002 onwards were compared and found to be in very good agreement (Hovmoeller diagrams in Figure 9 and northern minus southern hemisphere TPW in Figure 10); nighttime records were compared to avoid issues with orbit drift in the NOAA satellites. The overall consistency of the long-term moisture record from HIRS with the more recent ten-year record of Aqua MODIS brings added confidence to the atmospheric moisture determinations from both sensor systems.

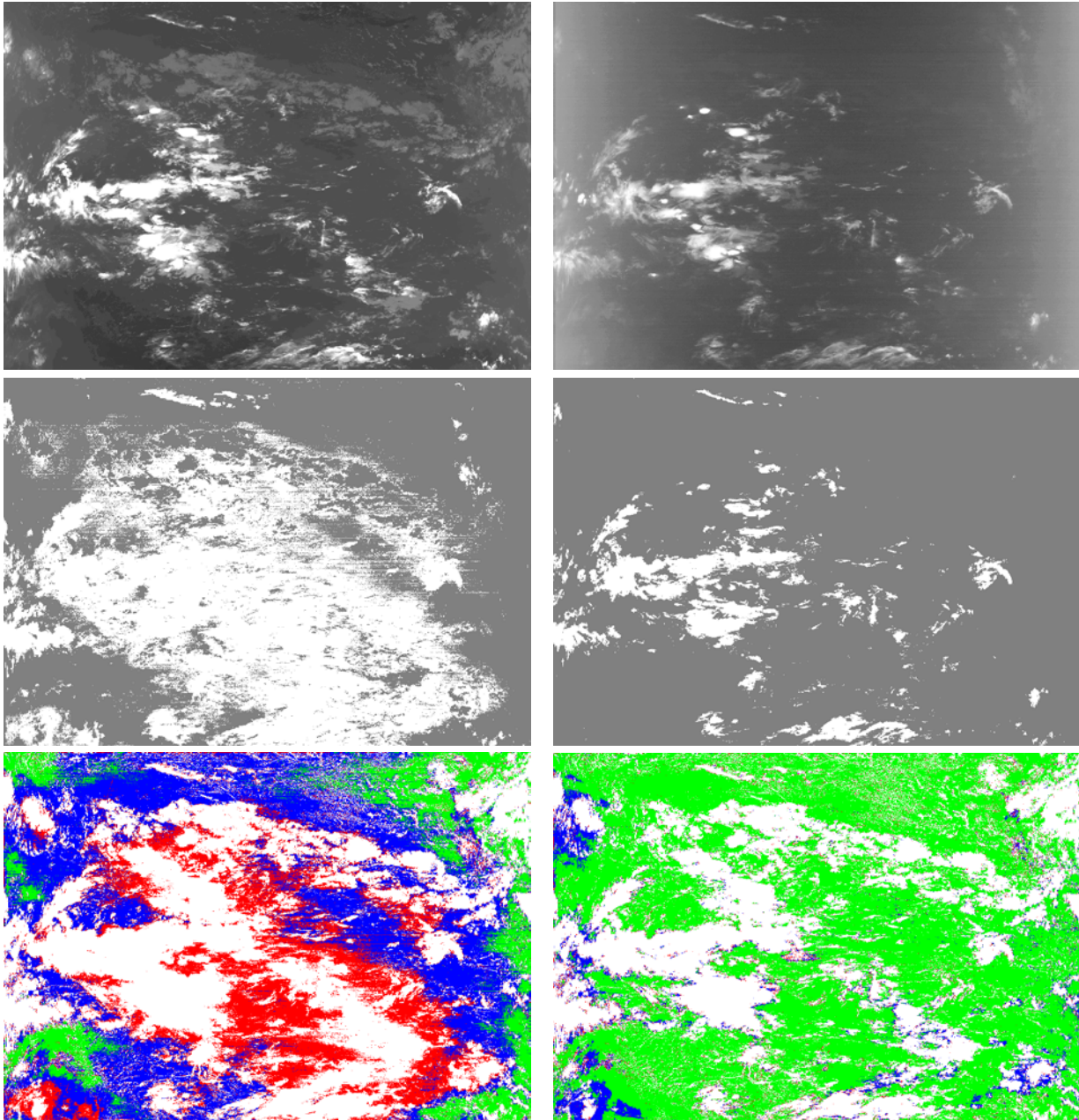
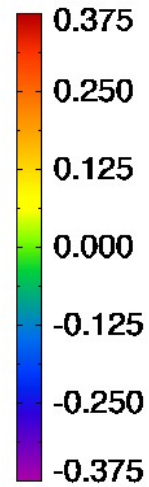
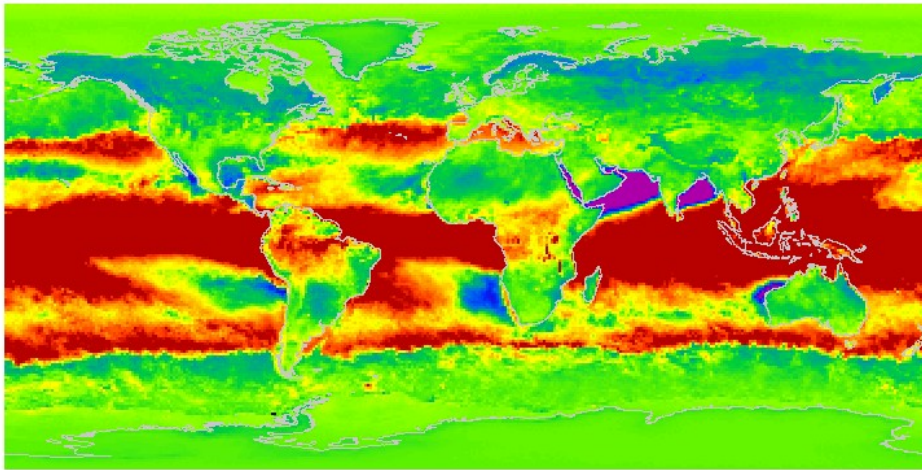


Figure 7 MODIS granule from 31 March 2014 at 05:30 UTC. Parts a, b are MODIS bands 31, 35 (11.1, 13.9 μm), parts b, c show results of 8.6-11.1 μm BTD ice phase cloud test for pre- and post- crosstalk calibration correction, parts e,f are final mask results for pre- and post- crosstalk calibration correction. See text for color definitions

Atmospheric_Water_Vapor_Mean_Mean

AS 1475 - 6



Test Data - Baseline Data

units = "cm"

Figure 7 Terra TPW test minus baseline. The purple negative differences may be due to the presences of dust or pollution or dry air blowing from the land.

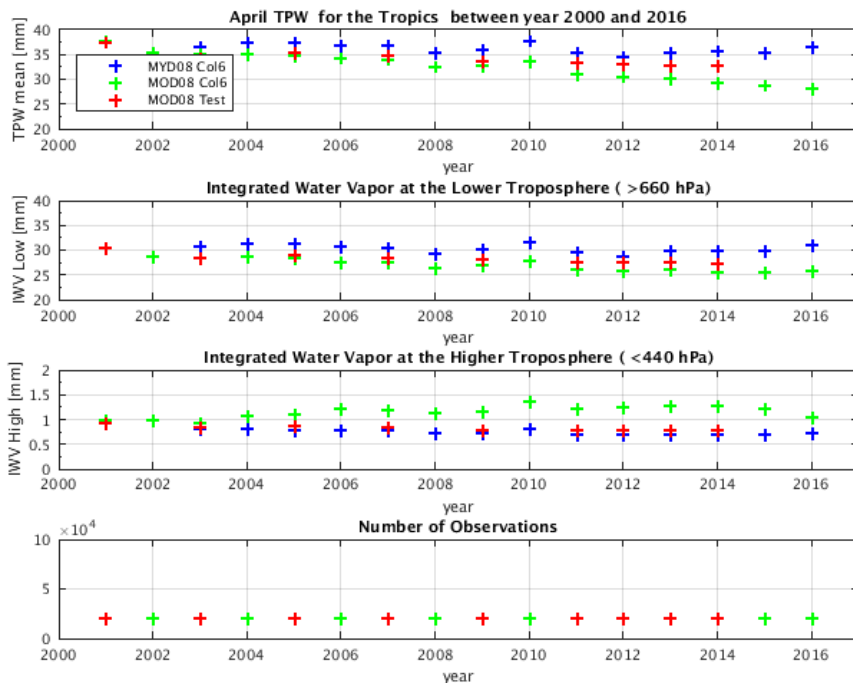


Figure 8 April Terra (MOD) and Aqua (MYD) tropical moisture (TPW, UTH, LTH) comparisons for current and test Terra cross-talk re-calibrations. The cross-talk correction is moving the Terra moisture products in better agreement to the Aqua determinations (especially for UTH).

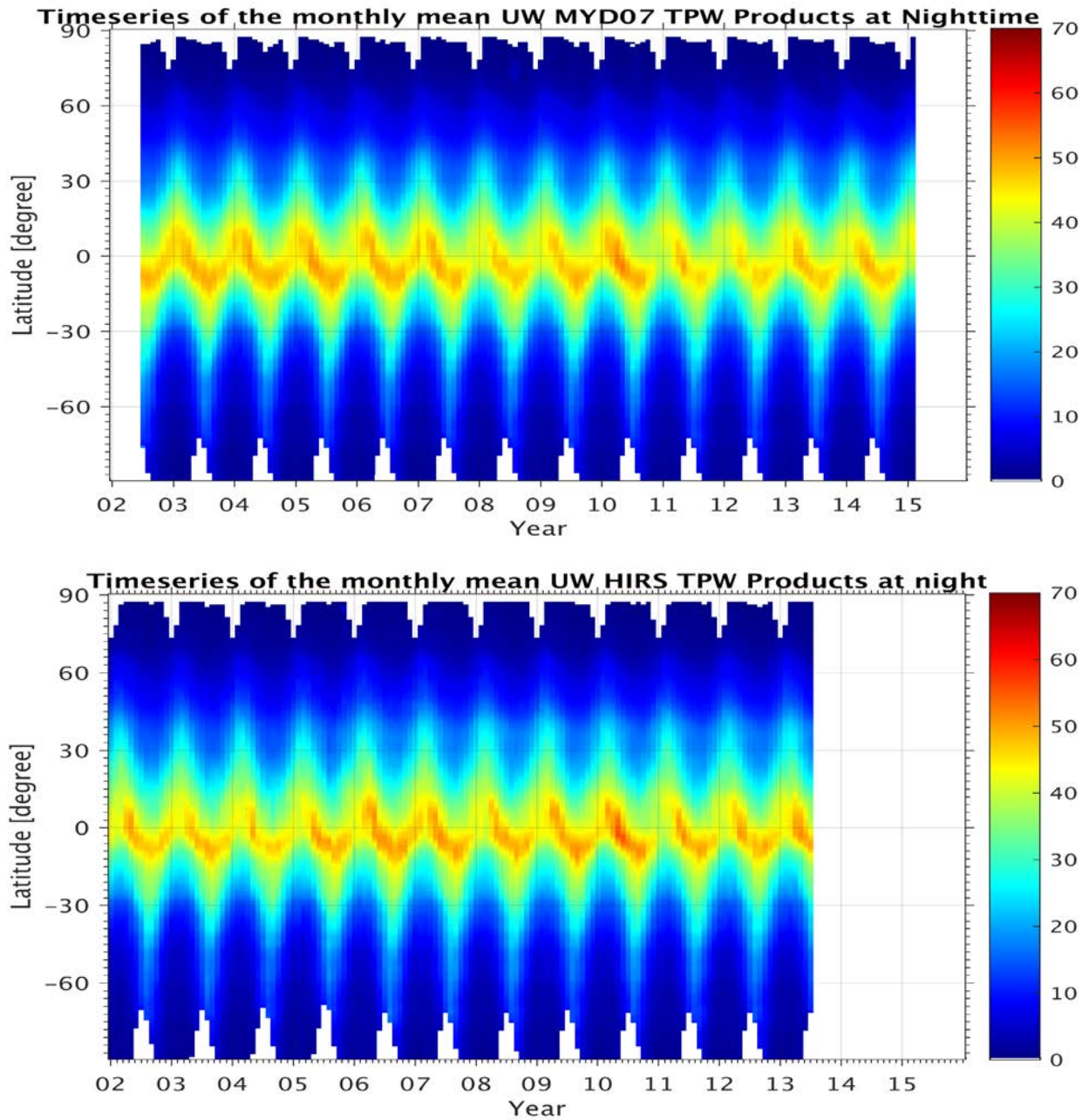


Figure 9 Aqua MODIS (top) and NOAA-16, -18, & -19 HIRS (bottom) Hovmoeller diagrams of nighttime TPW (in mm) for 2002 to 2015.

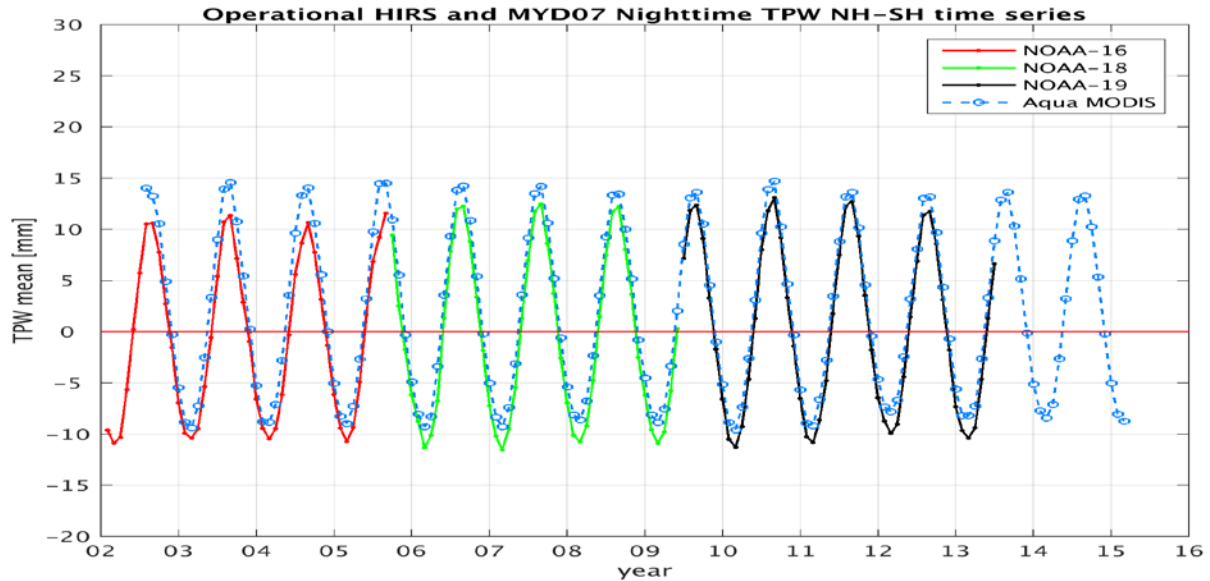


Figure 10 MODIS and HIRS Northern Hemisphere minus Southern Hemisphere TPW differences for 2002 to 2015. Note the somewhat greater detection of moisture in the northern hemisphere annually.

Cloud Top Heights and Phase (MOD06/MYD06)

MODIS and HIRS cloud property determinations were also compared. HIRS high clouds are determined using CO₂ slicing to estimate cloud top pressure for HIRS FOVs within 32 degrees of nadir over land and ocean both day and night. The retrieval approach is borrowed from MODIS (Menzel et al. 2008). High, mid, and low clouds are separated into thin, thick, and opaque categories. There is strong reliance on radiances from 13.3 to 14.2 μm . The AVHRR based PATMOS-x cloud mask is used to characterize HIRS sub-pixel cloud cover. The overall consistency of the long term high cloud frequency of detection record evident in the Hovmoeller diagrams from 2002 onwards (Figure 11) and the consistency in the northern minus southern hemisphere high cloud frequency of detection (Figure 12) also brings added confidence to the cloud determinations from both sensor systems. The HIRS high cloud trends were reported in Menzel et. al. (2016).

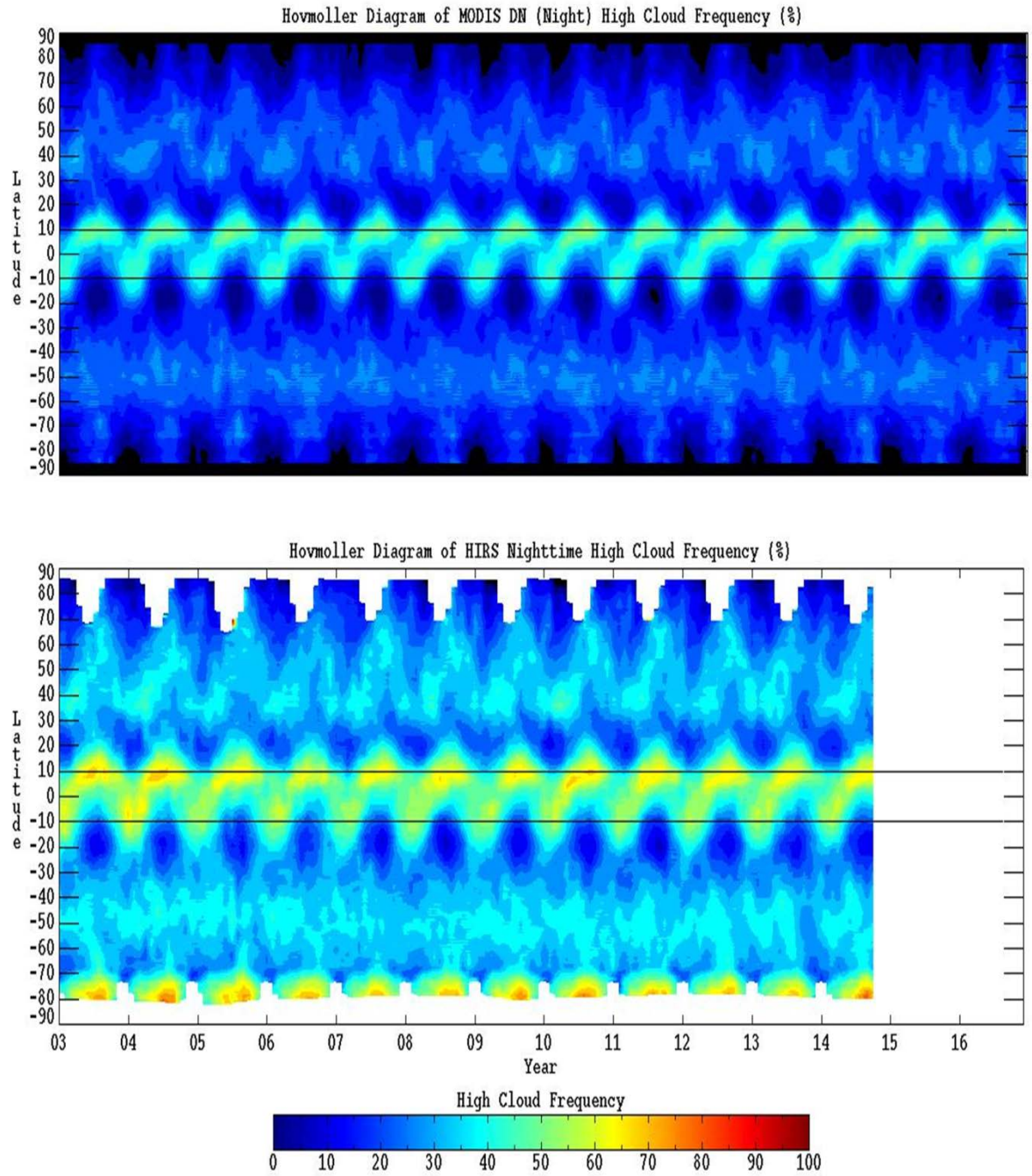


Figure 11 Aqua MODIS (top) and NOAA-16, -18, &-19 HIRS (bottom) Hovmoeller diagrams of nighttime high cloud frequency of detection (in %) for 2002 to 2015.

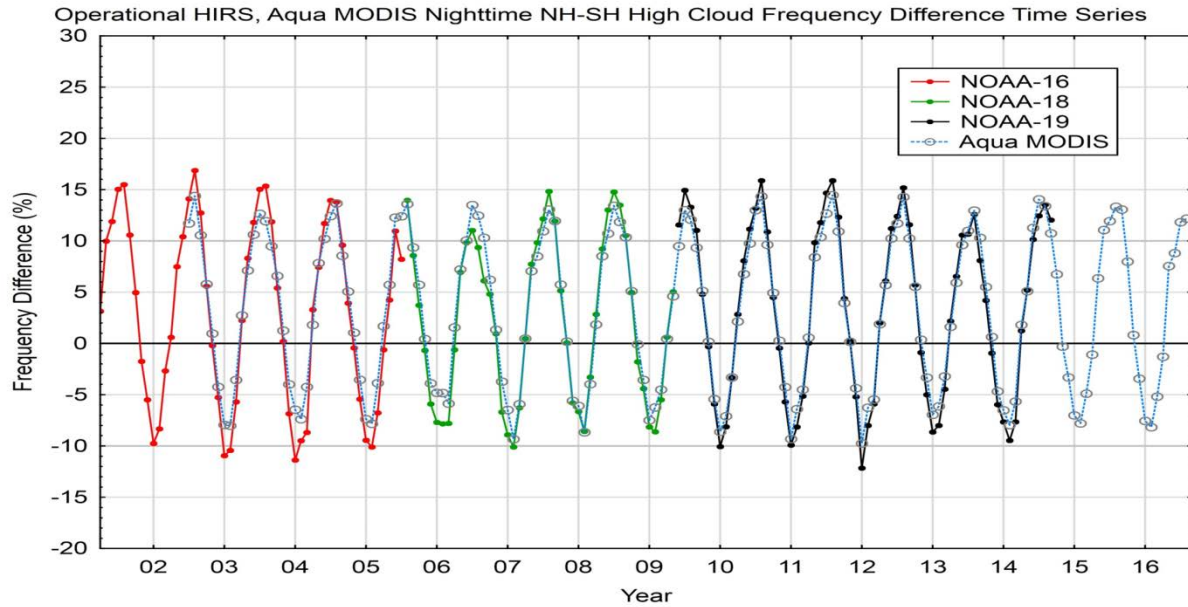


Figure 12 MODIS and HIRS Northern Hemisphere minus Southern Hemisphere high cloud detection frequencies for 2002 to 2015. The Northern Hemisphere peak cloudiness is roughly 5% greater annually.

MODIS Collection Pixel Level Comparison

One way to assess the impact of algorithm and calibration changes in a MODIS Collection is to compare pixel-level (i.e., instantaneous retrievals) products between two concurrent Collections. A recent study (Yi et al., 2017a) compared the collection 5.1 and collection 6 cloud physical and optical properties retrieved from Aqua MODIS pixel-level (i.e., Level 2) products in 2012. The primary objective was to determine what differences emerged during the data collection change for the general users of the MODIS ice and liquid water cloud products. The C6 to C51 comparisons were based on examination of two cases: (1) when cloud retrievals for a given pixel were valid simultaneously in both C51 and C6; and (2) when all valid cloud retrievals were considered in their respective collections. The selected pixels for each day in 2012 were first aggregated and gridded in daily half-degree resolution equal-angle grid boxes, and then further averaged annually, zonally, and globally.

One of the significant changes in Collection 6 was the transition from an ice model that assumed smooth surfaces (Collection 5) to an ice model that adopted severe roughening (Collection 6). For the Case 1 ice cloud comparisons, systematic increases were found in the C6 CER of about 6.68 μm globally. Spatial differences in CER also contributed to differences in the variation of zonal averaged values. The C51 COT was globally larger than the C6 COT by about 25%. While the CER and COT changed individually, the calculation of ice cloud water path derives from the multiplication of the two properties, which tend to offset each other so that the C51 and C6 ice

CWP are quite similar. The ice cloud-top height, increased slightly in the transition from C51 to C6. Low-level water cloud top heights decreased in regions of persistent stratocumulus where temperature inversions are prevalent, with results better in line with CALIPSO retrievals.

Yi et al. (2017b) investigated the impact of these cloud property differences between collections on the inference of cloud radiative effects (CREs). This question was addressed from a modeling perspective using one year (2012) of MODIS gridded, annually-averaged ice/liquid water cloud properties at $0.5^\circ \times 0.5^\circ$ spatial resolution. The Rapid Radiative Transfer Model for GCM (RRTMG) applications was used to simulate the broadband radiative fluxes at the top of the atmosphere under clear-sky and cloudy-sky conditions. The shortwave, longwave, and net radiative effects of ice, liquid water, and total clouds were derived individually assuming different cloud optical property parameterization schemes. The results provided ice and liquid water cloud CRE contributions to the total CRE. Significant differences were found in the simulated CREs between C6 and C51 for ice clouds (up to 23 W m^{-2} for the shortwave CRE) and liquid water clouds (approximately -4.5 W m^{-2} for the shortwave CRE). The C6 total CRE provided the closest match with the Cloud and the Earth's Radiant Energy System (CERES) Energy Balanced And Filled (EBAF) product.

Studies like these provide the community some necessary insight as to what sort of impact might be expected when a new Collection is made available, and also provide guidance on where further work remains to be done.

Work Plan

Continue monitoring performance of all relevant algorithms, including instrument performance, making adjustments as appropriate. Prepare for re-processing of Terra data to account for calibration adjustments.

References

- Ackerman, S.A., R.E. Holz, R. Frey, E.W. Eloranta, B.C. Maddux, and M. McGill, 2008: Cloud Detection with MODIS. Part II: Validation. *J. Atmos. Oceanic Technol.*, 25, 1073–1086.
- Di Girolamo, L., A. Menzies, G. Zhao, K. Mueller, C. Moroney, and D.J. Diner, 2010: Multi-angle Imaging SpectroRadiometer Level 3 Cloud Fraction by Altitude Algorithm Theoretical Basis Document. JPL Publ., D-62358, 23 pp.
- Heidinger, A. K., M. J Foster, A. Walther and X. Zhao, 2013: The Pathfinder Atmospheres Extended (PATMOS-x) AVHRR Climate Data Set. *Bull. Amer. Meteor. Soc.*, 95, 909–922. doi: <http://dx.doi.org/10.1175/BAMS-D-12-00246.1>
- Karlsson, K.-G., Anttila, K., Trentmann, J., Stengel, M., Meirink, J. F., Devasthale, A., Hanschmann, T., Kothe, S., Jääskeläinen, E., Sedlar, J., Benas, N., van Zadelhoff, G.-J., Schlundt, C., Stein, D., Finkensieper, S., Håkansson, N., and Hollmann, R.: CLARA-A2: The second edition of the CM SAF cloud and radiation data record from 34 years of global AVHRR data, *Atmos. Chem. Phys. Discuss.*, doi:10.5194/acp-2016-935, in review, 2017.
- Menzel, W. P., R. A. Frey, E. E. Borbas, N. Bearson, B. Baum, R. Chen, C. Cao, 2014: Recalibrating HIRS Sensors to Produce a 30 year Record of Radiance Measurements. Proceedings of the EUMETSAT Meteorological Satellite Conference, Geneva, Switzerland, 22-26 September, 2014.
- Menzel, W. P., R. A. Frey, E. E. Borbas, B. A. Baum, G. Cureton, and N. Bearson, 2016: Reprocessing of HIRS Satellite Measurements from 1980-2015: Development Towards a Consistent Decadal Cloud Record. *Jour. Appl. Meteor. Clim.* 55, 2397-2410. doi:10.1175/JAMC-D-16-0129.1
- Minnis, P., Q. Trepte, S. Sun-Mack, Y. Chen, D. R. Doelling, D. F. Young, D. A. Spangenberg, W. Miller, B. A. Wielicki, R. Brown, S. Gibson, and E. B. Geier 2008: Cloud Detection in Nonpolar Regions for CERES Using TRMM VIRS and Terra and Aqua MODIS Data, *IEEE Trans. Geosci. Remote Sens.*, 10.1109/TGRS.2008.2001351
- Minnis, P., K. Bedka, Q. Trepte, C. R. Yost, S. T. Bedka, B. Scarino, K. Khlopenkov, and M. M. Khaiyer, 2016: A consistent long-term cloud and clear-sky radiation property dataset from the Advanced Very High Resolution Radiometer (AVHRR). Climate Algorithm Theoretical Basis Document (C-ATBD), CDRP-ATBD-0826 Rev 1 AVHRR Cloud Properties - NASA, NOAA CDR Program, 19 September, 159 pp., DOI:10.789/V5HT2M8T.

- Moeller, C., R. Frey, E. Borbas, P. Menzel, T. Wilson, A. Wu, and X. Geng, 2017: Improvements to Terra MODIS L2 science products through using crosstalk corrected L1B radiances. Submitted to EOSXXII, SPIE, 2017.
- Trepte, Q. Z., P. Minnis, C. R. Trepte, S. Sun-Mack, and R. Brown, 2010: Improved cloud detection in CERES Edition 3 algorithm and comparison with the CALIPSO Vertical Feature Mask. Proc. AMS 13th Conf. Atmos. Rad. and Cloud Phys., Portland, OR, June 27 – July 2, JP1.32.
- Wilson, T., A. Wu, A. Shreshta, X. Geng, Z. Wang, C. Moeller, R. Frey, and X. Xiong, Development and Implementation of an Electronic Crosstalk Correction for Bands 27-30 in Terra MODIS Collection 6. Submitted to Remote Sensing, 2017.
- Winker, D. M., W. Hunt, and M. J. McGill, 2007: Initial performance assessment of CALIOP. Geophys. Res. Lett., 34, L19803, doi:10.1029/2007GL030135.
- Wylie, D. P., D. L. Jackson, W. P. Menzel, and J. J. Bates, 2005: Global Cloud Cover Trends Inferred from Two decades of HIRS Observations. J. Clim., 18, 3021–3031.
- Yi, B., A. D. Rapp, P. Yang, B. A. Baum, and M. D. King, 2017a: A comparison of Aqua MODIS ice and water cloud physical and optical properties between Collection 6 and Collection 5.1. Pixel-to-pixel comparisons. J. Geophys. Res. Atmos., 122, doi:10.1002/2016JD025586.
- Yi, B., A. D. Rapp, P. Yang, B. A. Baum, and M. D. King, 2017b: A comparison of Aqua MODIS ice and water cloud physical and optical properties between Collection 6 and Collection 5.1. Cloud radiative effects. In press, J. Geophys. Res. Atmos., 122, doi:10.1002/2016JD025654.

Publications

- Foster, M. H.; Ackerman, S. A.; Bedka, K.; Frey, R. A.; Di Girolamo, L.; Heidinger, A. K.; Sun-Mack, S.; Maddux, B. C.; Menzel, W. P.; Minnis, P.; Stegel, M. and Zhao, G. State of the climate in 2015: Cloudiness. Bulletin of the American Meteorological Society, Volume 97, Issue 8, 2016, S28-S29.
- Menzel, W. P., R. A. Frey, E. E. Borbas, B. A. Baum, G. Cureton, and N. Bearson, 2016: Reprocessing of HIRS Satellite Measurements from 1980-2015: Development Towards a Consistent Decadal Cloud Record. Jour. Appl. Meteor. Clim. 55, 2397-2410. doi:10.1175/JAMC-D-16-0129.1

- Moeller, C., R. Frey, E. Borbas, P. Menzel, T. Wilson, A. Wu, and X. Geng, 2017: Improvements to Terra MODIS L2 science products through using crosstalk corrected L1B radiances. Submitted to EOSXXII, SPIE, 2017.
- Wilson, T., A. Wu, A. Shreshta, X. Geng, Z. Wang, C. Moeller, R. Frey, and X. Xiong, Development and Implementation of an Electronic Crosstalk Correction for Bands 27-30 in Terra MODIS Collection 6. Submitted to Remote Sensing, 2017.
- Yi, B., A. D. Rapp, P. Yang, B. A. Baum, and M. D. King, 2017a: A comparison of Aqua MODIS ice and water cloud physical and optical properties between Collection 6 and Collection 5.1. Pixel-to-pixel comparisons. *J. Geophys. Res. Atmos.*, 122, doi:10.1002/2016JD025586.
- Yi, B., A. D. Rapp, P. Yang, B. A. Baum, and M. D. King, 2017b: A comparison of Aqua MODIS ice and water cloud physical and optical properties between Collection 6 and Collection 5.1. Cloud radiative effects. In press, *J. Geophys. Res. Atmos.*, 122, doi:10.1002/2016JD025654.

Meetings

Steve Ackerman attended the CALIPSO and CloudSat Ten-Year Progress Assessment and Path-Forward Workshop, Paris, 8-10 June 2016, and presented a talk titled "Cloud Properties from MODIS and CALIOP"

Chris Moeller attended the MODIS Science Team mtg June 7-10, 2016 and presented a talk titled "Impact of Terra/MODIS PVLWIR Crosstalk on L1 and L2 Products" to plenary.

Chris Moeller attended the MODIS Calibration Workshop on June 6, 2016 and presented a talk on Terra MODIS crosstalk findings.